JCARME
ISSN: 2228-7922
Journal of Computational and Applied Research in Mechanical Engineering
Vol. 4, No. 1, pp. 67- 79, Autumn 2014
http://jcarme.srttu.edu

Experimental and numerical study of heat flux distribution in laser forming of bi-layer sheets

Mohammad Riahi[a], Mohamad Hoseinpour Gollo[b,*] and Seiied Nader Ameli Kalkhoran[a]

[a] *Faculty of Mechanical Engineering, Iran University of Science and Technology, Tehran, Iran*
[b] *Manufacturing Engineering Department, Shahid Rajaee Teacher Training University, Tehran, Iran*

Article info:
Received: 04/10/2013
Accepted: 15/07/2014
Online: 11/09/2014

Keywords:
Laser Forming,
Cermet,
Gaussian distribution,
Uniform distribution.

Abstract
Laser forming is a modern process which is mainly used for forming metals. Different Lasers are used in this regard that includes Nd: YAG and CO_2. In this study, forming bi-layer sheets of Aluminum/Ceramic by Laser was investigated. Furthermore, effect of Uniform and Gaussian heat flux distribution in different power, velocity, and beam diameters on bending angle was studied. FEM simulation indicated that, in the same conditions of analysis, Uniform heat flux distribution caused higher bending angle than Gaussian heat flux distribution. Moreover, the results showed that there was an optimum point at different speeds and laser beam diameters, at which the bending angle was maximum. In order to evaluating the numerical results, a set of experiments was conducted, which showed good agreement.

1. Introduction

Laser forming process is a new technique which is created by thermal stress throughout laser radiation [1]. A set of laser beam and workpiece parameters such as power, wave length, diameters, velocity of laser radiation, absorption coefficient, specific heat, conductivity, and expansion coefficient affects the forming procedure. For the first time, Vollertsen [2] and Geiger [3] have discovered and suggested three different mechanisms to express behavior of thermo-mechanical materials, which were temperature gradient mechanism (TGM), buckling mechanism (BM), and upsetting mechanism (UM). This method could be widely used in rapid prototyping, automotive manufacturing, aerospace, and ship building [4-5]. Figure 1 shows the scheme of sheet bending due to laser radiation.

Although in most studies sheet bending has been considered along a straight line, some investigations have concentrated on the production of different geometrical shapes like spherical [6], Sattler shape [7], and pipe bending [8- 9]. So far, different materials have been examined numerically and experimentally by laser forming process. Some of these materials are different types of steels [10- 12], Aluminum [13- 14], Titanium [15], Copper [16], Silicon [17], and Chromium [18].

[*] *Corresponding author*
Email address: m.hoseinpour@srttu.edu

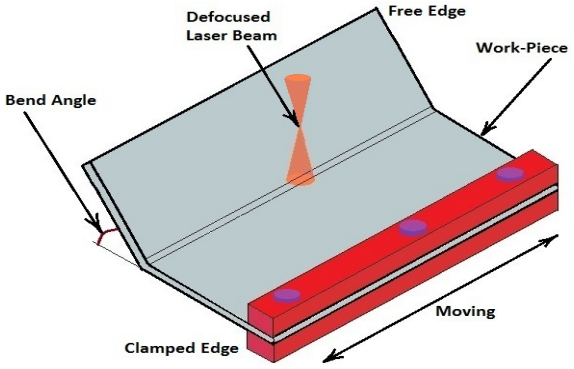

Fig. 1. Scheme of metal forming procedure using laser radiation.

Yao et al. [19] investigated laser forming of metal plates with pre-loads. For simulating this condition, the Gaussian heat distribution and nonlinear finite element analysis were used and showed that, when the pre-load was pure compression and pure bending (where e bending is toward the laser beam), the bending angle achieved the maximum amount. In the case of Uniform heat distribution, Hoseinpour Gollo et al. [20] presented a statistical analysis about effects of the parameters in laser forming of steel sheet metals and discovered an optimum condition in the forming process. In another investigation, Roohi et al. [21] used an external force in the laser forming of steel sheets by the Uniform heat distribution and found that nearly the two-third of bending angle amount was related to the external force. In a recent survey, Hoseinpour Gollo et al. [22] modeled closed cell foam and then simulated the laser forming process on it.

Bi-layer sheets are one of the most useful materials which can have many advantages such as stiffness, heat resistance, abrasion resistance, and corrosion resistance. The main downside of these materials is forming difficulties; if this drawback is overcome, they would be used more widely. In association with the forming of cermet sheet (Al/Sic) by laser forming process, Shen et al [23] performed a numerical study in 2009. This bi-layer cermet sheet combined the characteristics of Aluminum and Ceramic and, while having anti-erosion and strength capability of Ceramic, it also contained all natural properties of Aluminum. As mentioned, the principle disadvantage of this material was in its weak formability which caused a limitation in its utilization for a vast number of applications. Regarding the simulation of heat flux of laser radiation, different models have been recommended, the most recognized of which is Gaussian and Uniform heat distribution.

In this paper, for the first time, a comparison was made between the effects of Gaussian and Uniform heat distributions in the laser forming of Al/SiC bi-layer materials. Temperature distribution and plastic strain on the surface and thickness of the workpiece were the parameters that were scrutinized and studied herein. Results indicated that heat distribution was very close and almost equal on both Aluminum surfaces. However, due to low thermal diffusivity of ceramic, when the heat flux was applied to the cermet surface, the amount of temperature at the lower surface of ceramic layer was less than upper surface and, a short while later, the passage of laser radiation reached its maximum. In the end, in order to evaluate the simulation procedure, a set of experiments was done by a 300-watt Nd: YAG laser in "Chehreh Sazan Company".

2. Finite Element Simulation

2. 1. Geometry modeling

The material which was studied in this investigation was Al/ SiC bi-layer sheet; its dimension was 37.5×50mm and the thickness of metallic and ceramic layer was 0.2 and 0.4 mm, respectively. Figure 2 shows geometrical dimensions of the part. In this study, it was assumed that the primary workpiece was smooth and flat without any defaults.

2. 2. Material Properties

Another assumption which was made in the simulation was isotropic property of the workpiece. Since material properties are temperature-dependent, it is necessary for temperature-dependent properties to be defined. The mechanical model of the Aluminum layer was assumed to be elasto-

plastic and its amount at different temperatures is shown in Table 1.
According to the obtained results, the generated stress in the ceramic layer was always less than its yield stress. Therefore, this layer always remained in the elastic region. Consequently, the ceramic layer model was assumed to be perfect elastic. Properties of Aluminum and ceramic are given in Table 2.

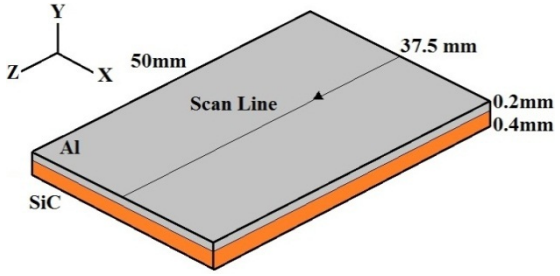

Fig. 2. Scheme of cermet piece.

Table 1. Temperature-dependent properties of Aluminum 6061 [24].

T(°C)	Yield stress (MPa)	T(°C)	Young's modulus (GPa)	T(°C)	Specific heat (J/Kg°C)	T(°C)	Density (Kg/m^3)	T(°C)	Conductivity (W/m°C)
20	125	20	70	20	898	20	2750	20	170
100	95	100	70	120	951	120	2730	585	220
200	55	200	61	220	1003	220	2710	---	---
300	27	300	55.6	320	1055	320	2690	---	---
400	15	400	49.3	420	1108	420	2660	---	---
500	5	500	41.3	587	1195	587	2630	---	---
600	5	600	5	644	1200	644	2450	---	---

Table 2. Properties o f Aluminum and ceramic [25, 26].

Properties	Al	SiC
Specific heat	898	630
Thermal conductivity (W/m°C)	170	0.32
Coefficient of thermal expansion (10^{-6}/°C)	23.65	3.8
Young's modulus (GPa)	70	450
Poisson's ratio	0.33	0.17
Yield strength (MPa)	125	-
Density	2750	3230

2. 3. Heat Flux Distribution

In the light of the fact that all the occurrence origins in a laser forming process is heat distribution, thus, review of all models of heat fluxes would be of high importance. Real model of heat distributing of laser radiation is close to Gaussian form (Fig. 3).
In this model, concentration of heat flux is in the center of radiation and, by moving away from it, the heat flux is exponentially decreased.

Mathematical equation of Gaussian heat flux distribution is as follows [14]:

$$I(x,y) = \frac{2P}{\pi r_0^2}\exp\left(\frac{-2\left[(x-x_0)^2+(y-y_0)^2\right]}{r_0^2}\right) \quad (1)$$

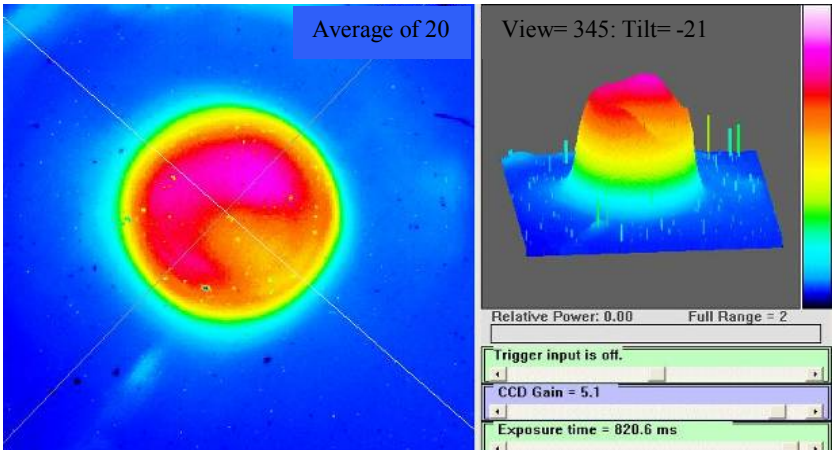

Fig. 3. Laser radiation profile in form of Gaussian distribution with 150 watt power.

In which P is the laser's power, r_o is the radius of laser beam, and (x_o, y_o) is coordinate of the laser beam center.

Uniform heat flux distribution is another model which has been used by some researchers to simulate the used heat flux of laser [20-21]. In this model, laser beam heat flux is applied to a surface with Uniform intensity. Equation of this type of heat flux distribution is:

$$I(x,y) = \frac{P}{\pi r_0^2} \qquad 0 \le r \le r_0 \qquad (2)$$

In the conducted numerical simulation, both types of heat fluxes were studied and their results were compared. Indeed, a very important point was to always maintain the part's temperature below its melting temperature. In this process, no external mechanical force was exerted on the part and also this part was assumed to contain no residual stress whatsoever.

2. 4. Boundary Conditions

In this process, one of the edges parallel to the scanning path of laser along Z direction was fixed. Boundary condition all over the surfaces of the part was assumed free convection, in which convection heat transfer coefficient was $12\,W/m°C$ and ambient temperature was $25\,°C$. The amount of heat transfer from the sheet's surfaces was according to the following equation:

$$q_c = h_c (T_s - T_0) \qquad (3)$$

In this equation, h_c is heat transfer convection coefficient, T_s is part's initial temperature, and T_0 is ambient temperature.

2. 5. Mesh Selection of Part

In all the conducted simulations, 3-D linear element and eight nodes (C38DT) were used. In order to increase the precision of the solution, meshing of the area affected by heat flux was selected as hexagonal below to reduce the analysis time of the software; further elements were selected as tetragonal and larger in dimensions. By changing the number of nodes and type of meshing, the analysis of mesh sensitivity was carried out. Overall, element number of the workpiece was equal to 19328. Figure 4 shows the meshing of the workpiece.

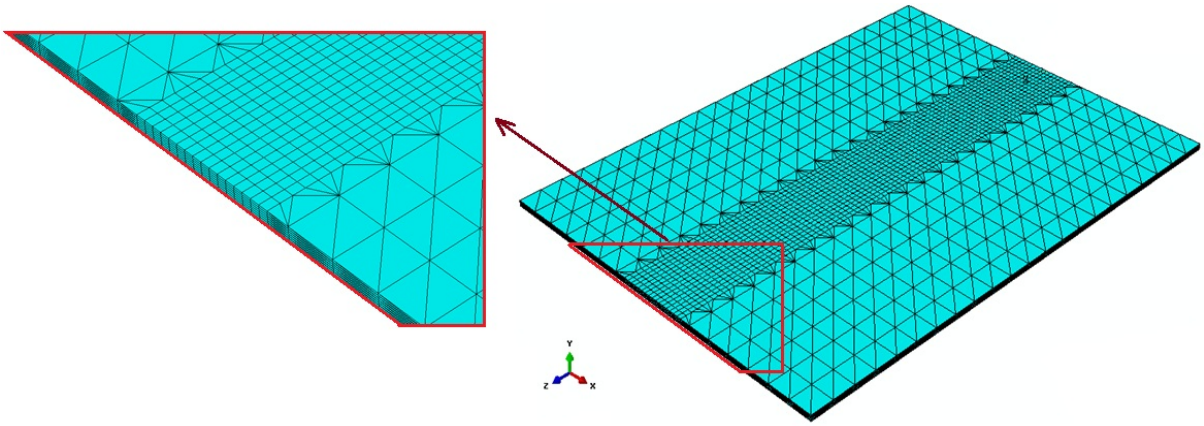

Fig. 4. Workpiece Meshing.

2. 6. Solution Condition

Solving this problem was in the form of coupled thermal-mechanical model. In order to increase the precision of analysis, nonlinear solution was used. Cooling time of the sheet after passing the laser radiation was assumed as 5 sec. This analysis, due to code writing in the sub-routine environment, had a one-step solution. Value of power, scanning speed, beam diameter, and path of scanning depending on the designated simulation were applied in the code writing section of the software. In solving this procedure, initially, heat analysis was done for each element by heat transfer relations. Afterward, the results were used for the mechanical-displacement analysis of that section.

3. Results and Discussion

It could be definitely stated that the main parameter in LF process is heat transfer and heat distribution. Therefore, studying these parameters is of utmost importance. In Fig. 5, temperature gradient of the workpiece along its thickness and at its center under Gaussian heat flux is shown.

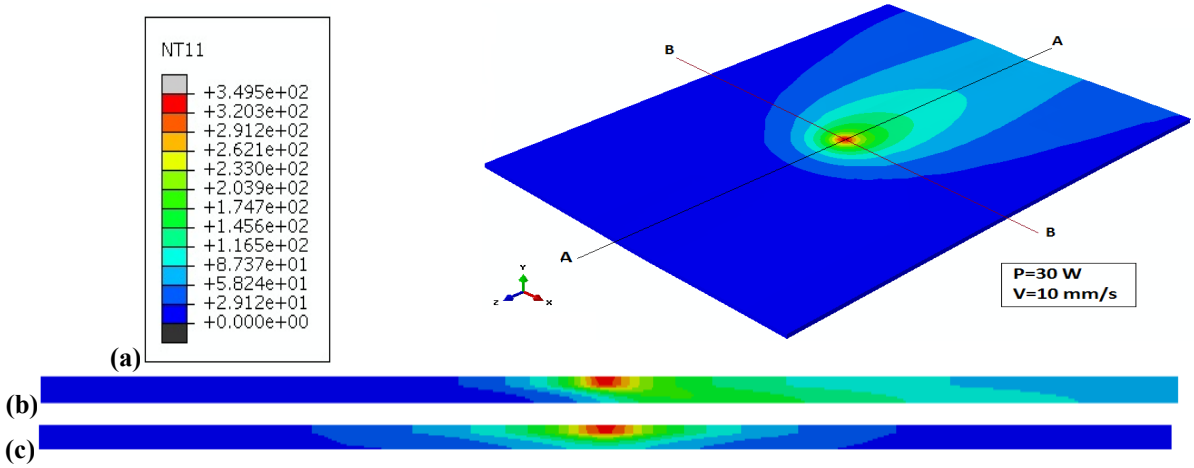

Fig. 5. (a). Temperature distribution by Gaussian heat flux, **(b).** Along AA and **(c).** Along BB.

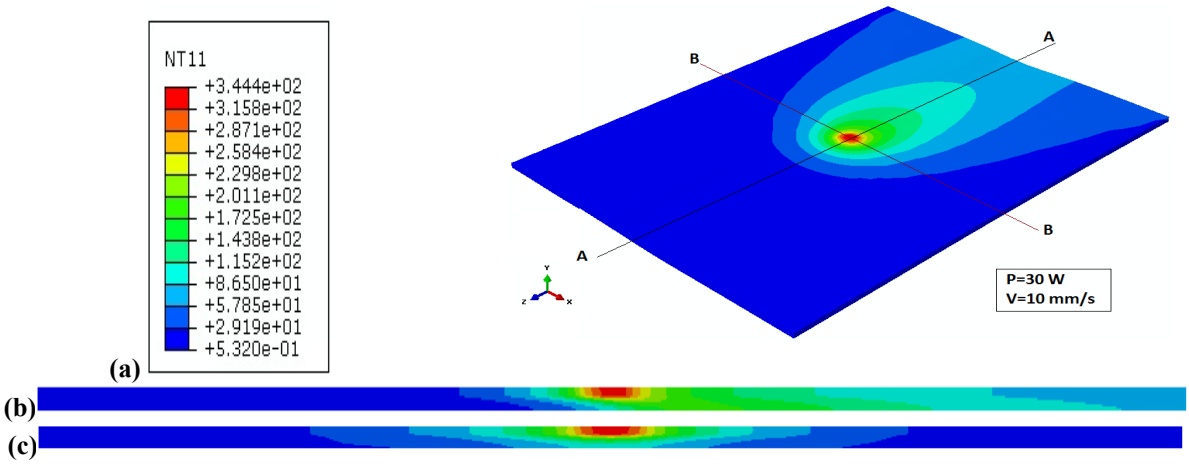

Fig. 6. (a). Temperature distribution by Uniform heat flux, **(b).** along A-A and **(c).** along B-B.

It is evident that maximum temperature was at the surface of the workpiece at the center of laser radiation. Also in this place, temperature gradient at the upper layer that was made of Aluminum was negligible. Probably, this issue was stemmed from the fact that this layer's thickness was very thin and the concentration of heat flux was minute. Passing of this layer, due to ceramic's low conductivity and temperature at the lower surface, dropped intensely.

In Fig. 6, heat distributing along the same direction is shown for Uniform heat flux. It is noticeable that maximum temperature of both conditions was almost equal. However, area of maximum temperature surface in Uniform heat flux was larger than that of Gaussian heat flux, which could be in the concentration of heat flux of Gaussian distribution in an area smaller than the diameter of laser radiation.

Temperature distribution on the surface of the workpiece and at different stages of the process for two assumed types of heat flux is shown in Fig. 7. Heat distribution at the workpiece's surface for both heat fluxes was almost equal. However, area of surface with maximum temperature was larger in the Uniform heat flux.

The main difference between Gaussian and Uniform heat flux was in the produced bending angle in the workpiece. Figure 8 shows plastic deformations at different stages which were induced by the passing of laser flux. Obtained results under different conditions including change in power, scanning speed, and laser beam diameter indicated the point that sheet plastic deformation under Uniform heat flux always was more than its value in the laser with Gaussian heat flux distribution.

Figures 9 and 10 depict changes in the bending angle of the sheet in laser forming process at different powers and scan speeds. Figure 9 shows that, with increasing the laser's power, sheet's bending angle also increased, which could be because by increasing the laser power, the temperature of upper surface increased, while the temperature of lower surface remained the same due to ceramic's low conductivity. As a result, the yield strength of upper layer dramatically dropped and the compressive stresses around this zone led to further bending in the workpiece. Figure 10 represents the presence of optimized point for bending angle at different speeds of laser scanning. The reason for decrease in bending angle at speeds higher than the optimized one was related to the decrease in heat gradient along thickness. By reducing the scanning speed, it could be definitely stated that the whole sheet thickness was equally heated in the scanning location. As a result, heat gradient and subsequently its bending angle decreased.

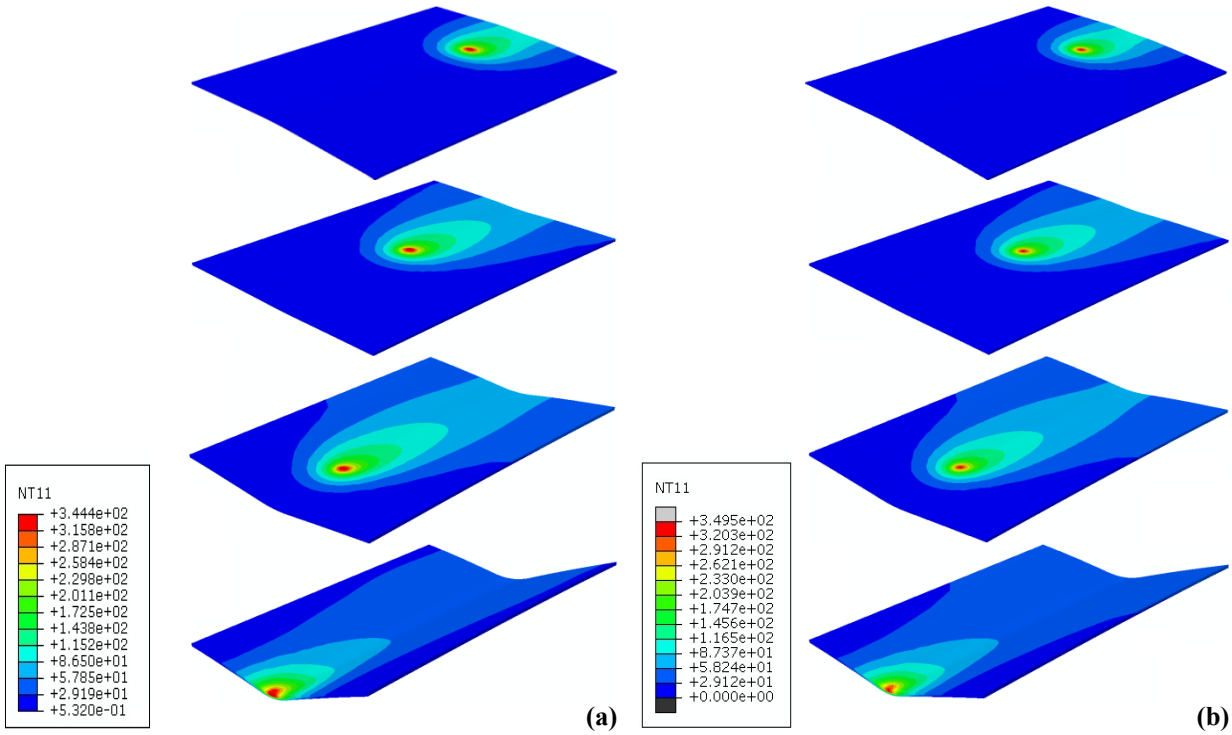

Fig. 7. Heat distribution on the surface of the workpiece in different stages; **(a).** for Uniform heat flux and **(b).** for Gaussian heat flux (P=30w, V=10mm/s).

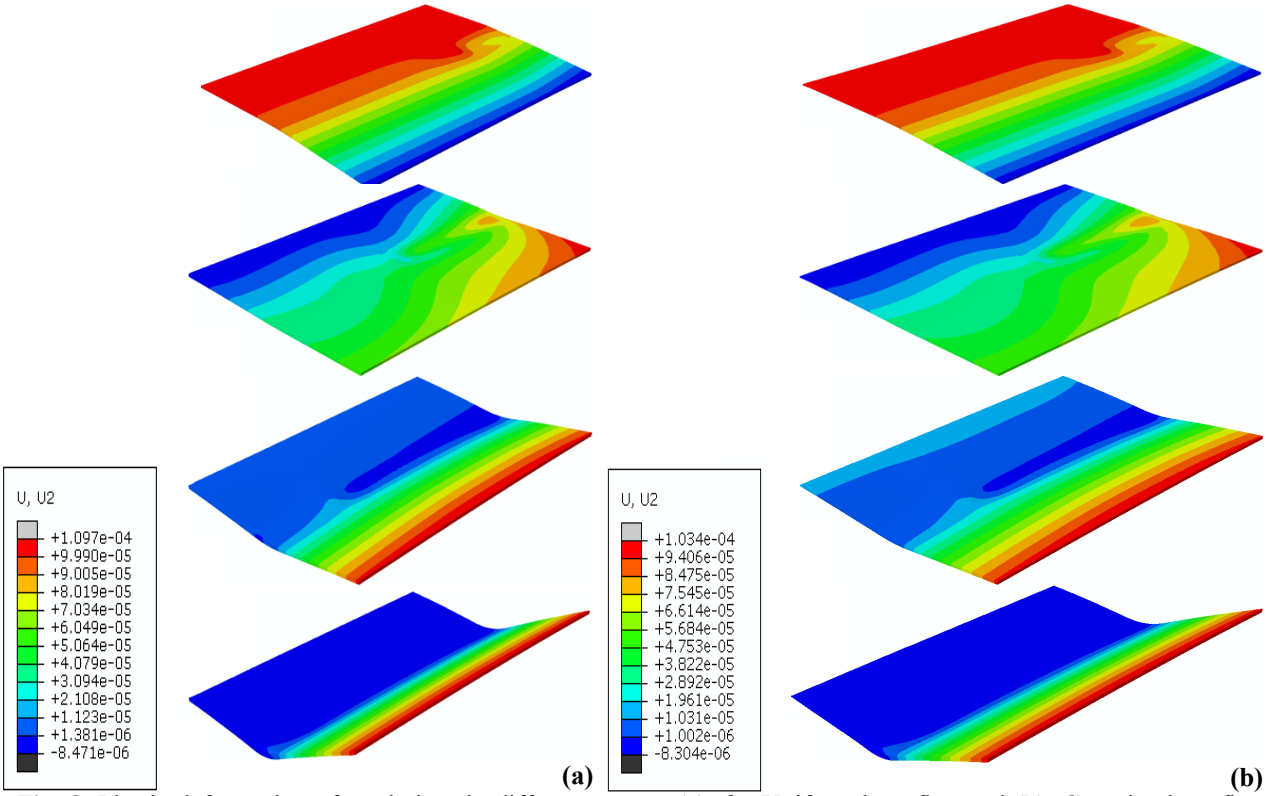

Fig. 8. Plastic deformation of workpiece in different stages; **(a).** for Uniform heat flux and **(b).** Gaussian heat flux (P=30W, V=10mm/s).

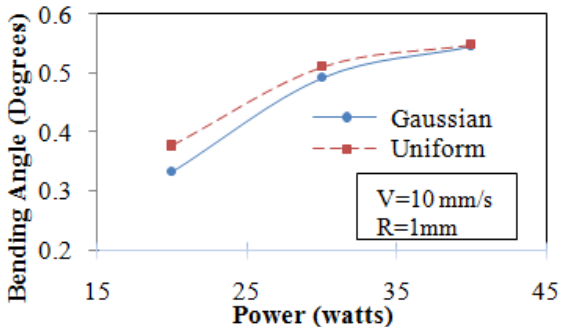

Fig. 9. Changes in bending angle for Gaussian and Uniform distribution of laser heat flux in different laser powers.

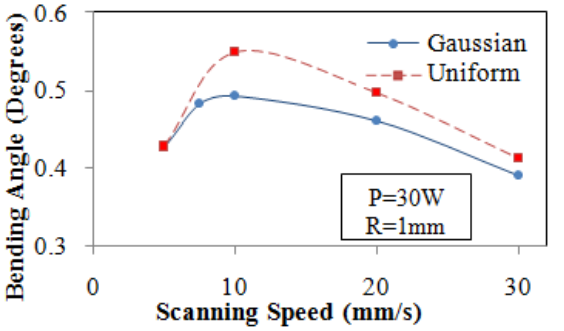

Fig. 10. Changes in bending angle for Gaussian and Uniform distribution of laser heat flux in different scanning speeds of laser.

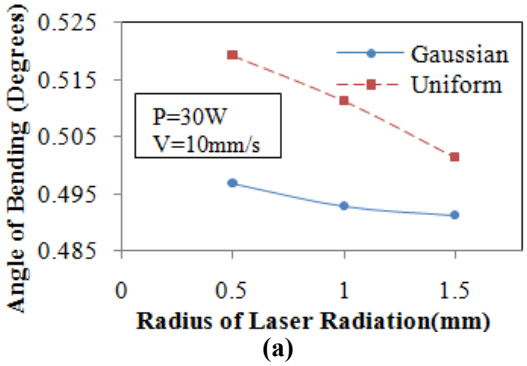

(a)

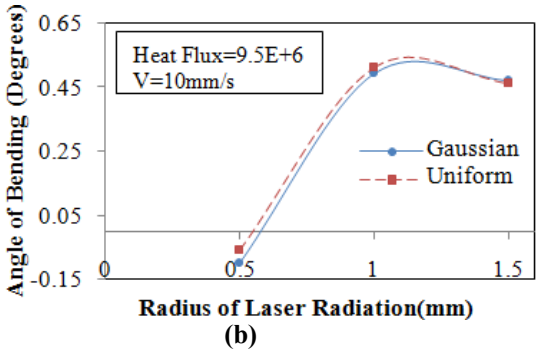

(b)

Fig. 11. Changing in bending angle for Gaussian and Uniform distribution in different laser beam diameter. **(a).** In constant power condition, **(b).** In constant heat flux.

Figure 11 shows changes in bending angle caused by different laser beam diameters. In Fig. 11(a), by keeping the speed and power of laser fixed, laser beam diameter changed and bending angles were obtained under two types of Gaussian and Uniform heat flux. It is evident that increasing beam diameter in both types of heat distribution caused reduction in the bending angle, because despite enlargement in beam diameter, the same constant power was applied to a larger area and hence reduction in heat gradient and subsequently decrease in the final bending angle were deduced. In Gaussian heat distribution, maximum generated heat was concentrated in the center of radiation. For this reason, in comparison with Uniform heat distribution, a smaller area would be involved in the procedure of plastic deformation and thus the produced bending angle would be smaller.

Figure 11(b) shows a different result from the previous case. In this condition, since heat flux was constant, by increasing laser beam, more heat power would be applied to the surface. As a result, heat stress and thus heat strain increased and eventually larger bending angle was obtained. Also, if heat power surpassed its optimized point, heat distribution along sheet thickness would become smoother and heat gradient would decrease. Consequently, the final bending angle also decreased.

In order to study temperature distribution at different points of the workpiece, the defined paths in Fig. 12 were selected. Values related to Gaussian and Uniform heat flux distributions just when laser beam scanned exactly half of the path, has been shown in Fig. 13.

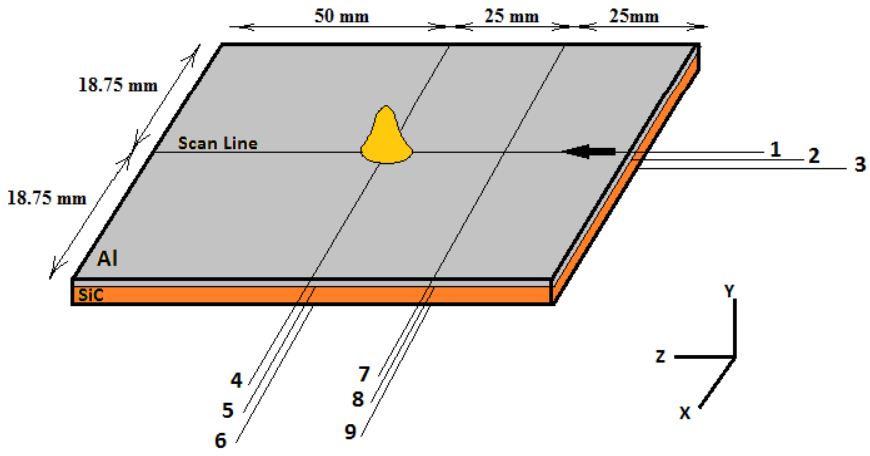

Fig. 12. Studied paths of temperature distribution.

As far as the three paths of 1, 2, and 3 were concerned, as was expected, maximum temperature was along path 1. However, due to low thickness of Aluminum layer, it is evident that heat gradient in this layer was negligible and temperature of upper and lower surfaces of this layer was the same almost along all path length (paths 1 and 2). On the other hand, since lower ceramic layer had less conductivity, heat along thickness of this layer transferred slower and, for this reason, the lower surface (path 3) reached its maximum temperature a short time after the pass of laser radiation from its upper surface.

Because of the symmetric conditions in paths 4 - 9, diagrams were also symmetric. Comparing two types of heat flux in these paths made it evident that these heat diagrams under Uniform heat flux were almost 5% wider than those obtained from Gaussian heat flux and their maximum temperature was on average 6% larger; larger area of maximum heat flux in Uniform heat distribution could be mentioned as the reason. Similar to the analysis provided in the case of path 3, as expected, temperature of path 6 was less than that of the two upper surfaces and temperature of path 9 was more than its two upper surfaces.

4. Validation

Due to the limitation in the availability of the Cermet sheet, experimental tests were done for bi-layer Fe/Al with the total thickness of 2.105mm and dimensions of 60×105 mm^2. Thickness of each layer was measured by an optic microscope that is shown in Fig. 14. Thickness of Fe layer was 1.455mm and that of Al layer was 0.650 mm.

For forming this sheet, Nd: YAG laser, model HAN*S LASER with the maximum power of 300W was used. The available ranges for the laser parameters were 1–1000 Hz for pulse frequency, 0.02-20 ms for pulse duration, and 0–30 J for pulse energy. The experiments were conducted with frequency of 29 Hz and workpiece velocities of 7 mm/s. Two major factors were important for selecting 29 Hz frequency: the first factor was the required overlapping of the alternative laser pulses regarding process travel speed and absolute irradiated energy per unit length of the workpiece. The second factor was limitations of laser source that confined the present choices about each combination of laser pulse energy, pulse duration, and frequency for each value of average output power.

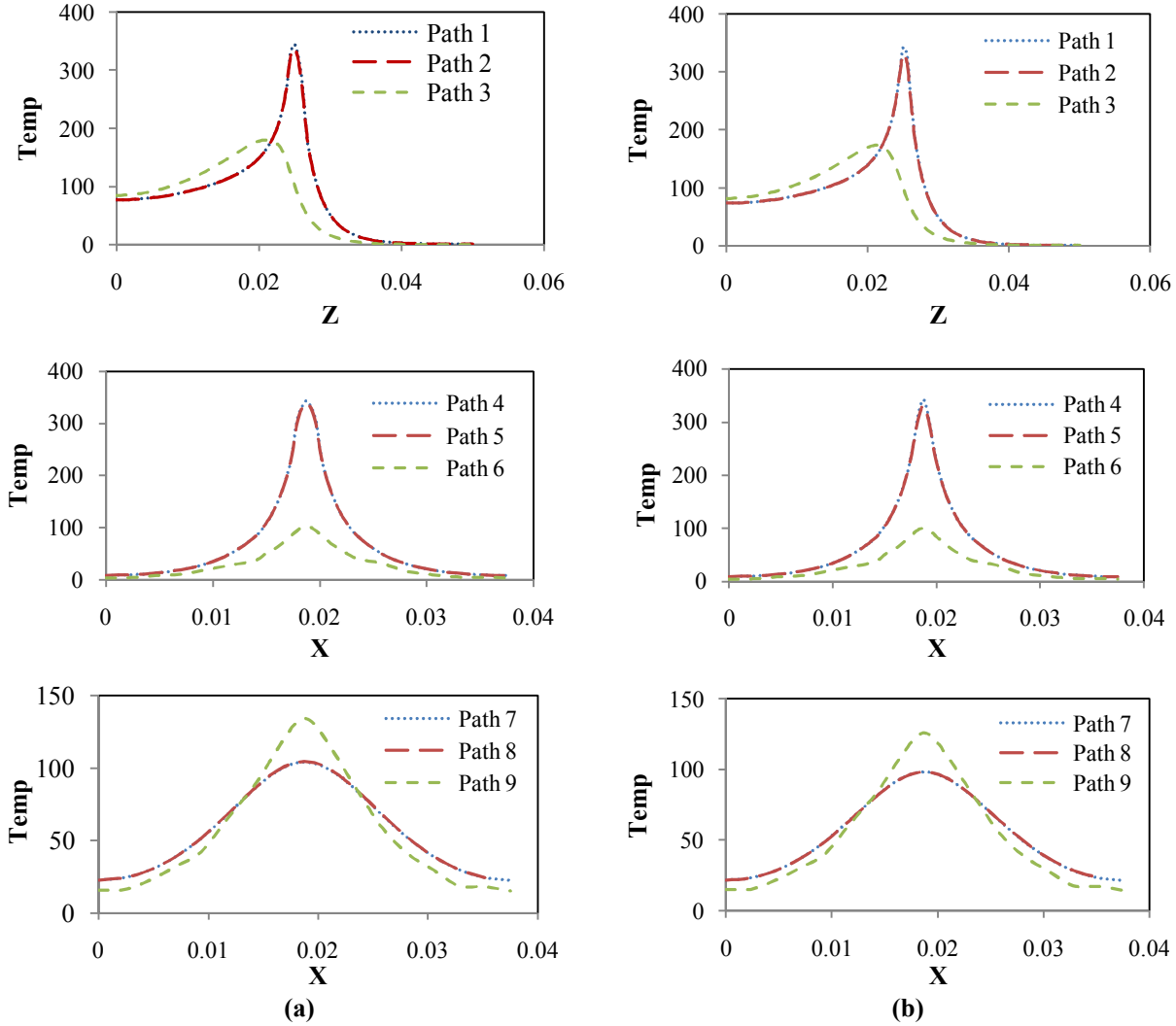

Fig. 13. Temperature distribution of the workpiece along different paths: **(a).** For Uniform heat flux, **(b).** for Gaussian heat flux.

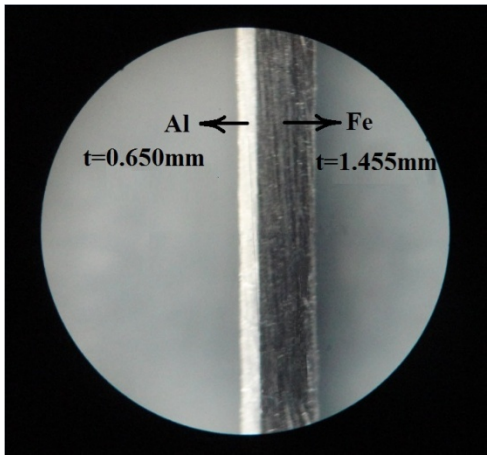

Fig. 14. An image of the sheet thickness.

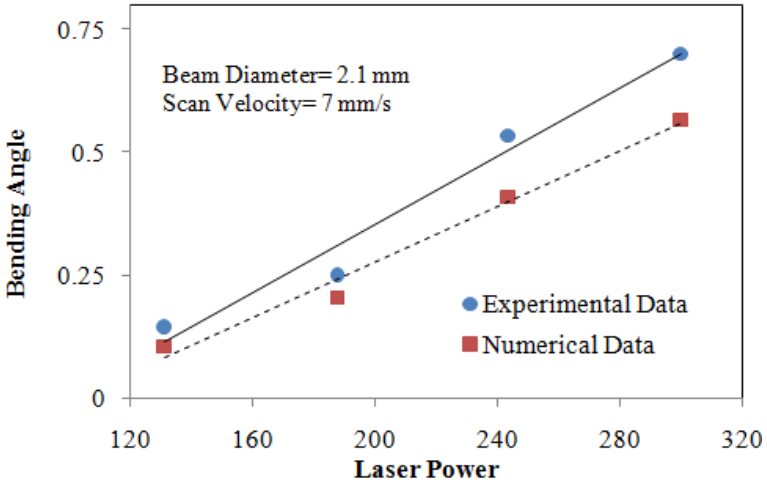

Fig. 15. Comparison between experimental and numerical results.

Result of the simulations and experimental tests for a laser with 2.1mm beam diameter and 11ms pulse duration with scan velocity of 7mm/sis shown in Fig. 15. These results demonstrated good agreement among the numerical and experimental data. Because of the thermal nature of this process, there was no crack in the formed work pieces in comparison with the traditional forming methods.

5. Conclusions

In this paper, effects of two types of Gaussian and Uniform laser heat flux on different parameters were presented. The following results were also obtained from this study:

- Uniform heat flux always produced larger bending angle compared with that of Gaussian distribution because of the larger radiation area at maximum heat flux.
- There was optimum velocity of laser beam, in which the bending angle was maximum, because first by reducing scanning speed, heat gradient in the sheet thickness increased. However, after a certain amount, its reverse occurred and bending angle decreased.
- At constant laser power, increasing in the beam diameter caused reduction in the bending angle.
- At constant heat flux, the bending angle raised by increasing the laser's beam diameter up to a certain amount. Afterward, by increasing beam diameter, trend of increase stopped and a mild decrease began. It was due to expansion at the surface temperature gradient and also changes in the nature of mechanism to BM.
- Temperature distribution of the workpiece in the Uniform flux condition was almost 5% wider than its amount in Gaussian flux.
- Maximum temperature of the workpiece in the Uniform heat flux distribution was nearly 6% higher on average.
- Comparison between experimental and numerical results showed good agreement between this set of data and rate of increase in bending angle was averagely 0.0038 °C/W.

6. References

[1] Y. Namba, "Laser forming in space", *Proceedings of International Conference on Lasers*, Las Vegas, pp. 403-407, (1985).

[2] K. Scully, "Laser line heating", *Journal of Ship Production*, Vol. 3, No. 4, pp. 237-246, (1987).

[3] Hong Shen and Frank Vollertsen, "Modeling of laser forming - An review", *Computational Materials Science*, Vol. 46, No. 4, pp. 834-840, (2009).

[4] J. Magee, "Laser bending of high strength alloys", *Journal of Laser Applications,* Vol.10, No. 4, pp. 149-155, (1998).

[5] G. Thomson and M. S. Pridham, "Controlled laser forming for rapid prototyping", *Rapid Prototyping Journal,* Vol. 3, No. 4, pp. 137-143, (1997).

[6] T. Hennige, "Laser forming of spatially curved parts", *Proceedings of the LANE,* pp. 409-420, (1997).

[7] J. Magee, K. G. Watkins and T. Hennige, "Symmetrical laser forming", *Proceedings of ICALEO*, pp. 77-86, (1999).

[8] N. Hao and L. Li, "An analytical model for laser tube bending ", *Applied Surface Science,* Vol. 208, No. 1, pp. 432-436, (2003).

[9] Shakeel Safdar, Lin Li, M. A. Sheikh and Zhu Liu, "Finite element simulation of laser tube bending: Effect of scanning schemes on bending angle, distortions and stress distribution", *Optics & Laser Technology,* Vol. 39, No. 36, pp. 1101-1110, (2007).

[10] M. Hoseinpour Gollo, H. Moslemi Naeini, G. H. Liaghat, M. J. Torkamany, S. Jelvani and V. Panahizade, "An experimental study of sheet metal bending by pulsed Nd: YAG laser with DOE method", *International Journal of Material Forming,* Vol. 1, No. 1, pp.137-140, (2008).

[11] L. J. Yang, J. Tang, M. L. Wang, Y. Wang and Y.B. Chen, "Surface characteristic of stainless steel sheet after pulsed laser forming", *Applied Surface Science,* Vol. 256, No. 23, pp. 7018-7026, (2010).

[12] B. S. Yilbas, A. F. M. Arif and B. J. Abdul Aleem, "Laser bending of AISI 304 steel sheets: Thermal stress analysis", *Optics & Laser Technology,* Vol. 44, No. 2, pp. 303-309, (2012).

[13] G. N. Labeas, "Development of a local three-dimensional numerical simulation model for the laser forming process of aluminium components", *journal of materials processing technology,* Vol. 207, No. 1-3, pp. 248-257, (2008).

[14] I. Pitz, A. Otto and M. Schmidt, "Simulation of the Laser Beam Forming Process with Moving Meshes for Large Aluminium Plates", *Physics Procedia,* Vol. 5, Part. B, pp. 363-369, (2010).

[15] D. P. Shidid, M. Hoseinpour Gollo, M. Brandt and M. Mahdavian, "Study of effect of process parameters on titanium sheet metal bending using Nd: YAG laser", *Optics & Laser Technology,* Vol. 47, No. 3, pp. 242-247, (2013).

[16] Chao Zheng, Sheng Sun, ZhongJi, Wei Wang and Jing Liu, "Numerical simulation and experimentation of micro scale laser bulge forming", *International Journal of Machine Tools & Manufacture,* Vol. 50, No. 12, pp. 1048-1056, (2010).

[17] WANG Xu-yue, XU Wei-xing, XU Wen-ji, HU Ya-feng, LIANG Yan-de and WANG Lian-ji, "Simulation and prediction in laser bending of silicon sheet", *Transactions of Nonferrous Metals Society of China,* Vol. 21, supplement 1, pp. 188-193, (2011).

[18] K. C. Chan, Y. Harada, J. Liang and F. Yoshida, "Deformation Behaviour of Chromium Sheets in Mechanical and Laser Bending", *Journal of Materials Processing Technology,* Vol. 122, No. 2-3, pp. 272-277, (2002).

[19] Zhenqiang Yao, Hong Shen, Yongjun Shi and Jun Hu, "Numerical study on laser forming of metal plates with pre-loads", *Computational Materials Science*, Vol. 40, No. 1, pp. 27-32, (2007).

[20] M. Hoseinpour Gollo, S. M. Mahdavian and H. Moslemi Naeini, "Statistical analysis of parameter effects on bending angle in laser forming process by pulsed Nd: YAG laser", *Optics & Laser Technology,* Vol. 43, No. 3, pp. 475-482, (2011).

[21] Amir H. Roohi, M. Hoseinpour Gollo and H. Moslemi Naeini, "External force-assisted laser forming process for gaining high bending angles", *Journal of Manufacturing Processes*, Vol. 14, No. 3, pp. 269-276, (2012).

[22] Mohammad Hosseinpour Gollo, Masoud Abbaszadeh and Iraj Mirzaee, "Geometrical modeling of closed-cell metal foams using Stochastic cells generation", *Modares Mechanical Engineering*, Vol. 14, No. 3, pp. 129-135 (2014). (In Persian)

[23] Hong Shen, Zhenqiang Yao and Jun Hu, "Numerical analysis of metal/ceramic bilayer materials systems in laser forming", *Computational Materials Science,* Vol. 45, No. 2, pp. 439-442, (2009).

[24] Xian Luo , Yanqing Yang, Jiankang Li, Meini Yuan, Bin Huang and Yan Chen, "An analysis of thermal residual stresses in SiC_f/Cu composites when TiC or Ni as binder", *Materials and Design,* Vol. 29, No. 9, pp. 1755-1761, (2008).

[25] S. G. Long and Y. C. Zhou, "Thermal fatigue of particle reinforced metal–matrix composite induced by laser heating and mechanical load", *Composites Science and Technology,* Vol. 65, No. 9, pp. 1391-1400, (2005).

[26] Jolanta Zimmerman, Wladyslaw Wlosinski and Zdzislaw R. Lindemann, "Thermo-mechanical and diffusion modeling in the process of ceramic–metal friction welding", *Journal of Materials Processing Technology,* Vol. 209, No. 4, pp. 1644-1653, (2009).